

Shannon entropy in confined He-like ions within a density functional formalism

Sangita Majumdar and Amlan K. Roy*

Department of Chemical Sciences

Indian Institute of Science Education and Research (IISER) Kolkata,

Mohanpur-741246, Nadia, WB, India

Abstract

Shannon entropy in position ($S_{\mathbf{r}}$) and momentum ($S_{\mathbf{p}}$) spaces, along with their sum (S_t) are presented for unit-normalized densities of He, Li⁺ and Be²⁺ ions, spatially confined at the center of an impenetrable spherical enclosure defined by a radius r_c . Both ground as well as some selected low-lying singly excited states, *viz.*, $1s_n s$ ($n = 2-4$) 3S , $1s_n p$ ($n = 2-3$) 3P , $1s3d$ 3D are considered within a density functional methodology that makes use of a work-function-based exchange potential along with two correlation potentials (local Wigner-type parametrized functional as well as the more involved non-linear gradient- and Laplacian-dependent Lee-Yang-Parr functional). The radial Kohn-Sham (KS) equation is solved using an optimal spatial discretization scheme via the generalized pseudospectral (GPS) method. A detailed systematic analysis of the confined system (relative to corresponding free system) has been performed for these quantities with respect to r_c in tabular and graphical forms, *with and without* electron correlation. Due to compression, the pattern of entropy in aforementioned states gets characterized by various crossovers at intermediate and lower r_c regions. The impact of electron correlation is more pronounced in weaker confinement limit, and appears to decay with rise in confinement strength. The exchange-only results are quite good to provide a decent qualitative discussion. The lower-bounds provided by entropic uncertainty relation holds good in all cases. Several other new interesting features are observed.

Keywords: Shannon Entropy, quantum confinement, impenetrable boundary, excited states, Helium-like ions, exchange-correlation.

*Corresponding author. Email: akroy@iiserkol.ac.in, akroy6k@gmail.com.

I. INTRODUCTION

A particle in an impenetrable box of infinite height has served the role of a simple, elegant pedagogical tool to illustrate the effects of boundary condition on energy spectrum of a quantum system. Understanding of such a system in some sub-region Ω of space (in contrast to “whole” space available in *free* system) offers new insights to simulate realistic situations in highly inhomogeneous media or in an external field. Matter constricted under such extreme pressure environment gives rise to a wide range of novel changes (from respective free counterpart) in energy spectra, electronic structure, chemical reactivity, ionization potential, polarizability etc., depending on *geometrical forms of cavity and dimensions*. This has inspired a variety of theoretical and experimental works. Some prominent applications are found in the context of cell model of liquid, superlattice structure, quantum dot, quantum wire, atoms/molecules encapsulated inside nanocavities (like fullerene, zeolite sieves, porous silicon, carbon nanotube), modelling defects in solids, confined phonons (or plasmons, polaritons, gas of bosons), as well as astrophysical phenomena such as mass-radius relation of white dwarfs, ionized plasma etc. The topic is vast and there has been a burgeoning growth of activity as evident from an extensive literature having many excellent comprehensive reviews. Interested reader may refer to following reviews [1–5] and references therein.

The first report of a confined hydrogen atom (CHA) within a sphere having rigid impenetrable walls was published as early as in 1937 [6] imposing the Dirichlet boundary condition that the wave function vanishes at boundary. Subsequently, many attempts have been made to estimate the eigenvalues and eigenfunctions invoking a wide range of approximate analytic, semi-analytic and purely numerical schemes. Here we mention a few ones like Rayleigh-Schrödinger perturbation theory, Wentzel-Kramers-Brillouin method, power-series solution, hypervirial theorem, Padé approximation, Lie algebraic treatment, super-symmetric quantum mechanics, Lagrange-mesh method, asymptotic iteration method, searching the zeros of hypergeometric function, generalized pseudospectral (GPS) method, Hartree-Fock (HF) method [7–22]. In recent years, exact solution of the Schrödinger equation has been found in terms of Kummer-M function (confluent hypergeometric) [16]. As the boundary approaches nucleus and volume of confinement squeezes, one notices a monotonic increase in energy in CHA. Another interesting feature is that, in contrast to free atom, due to breaking of symmetry in CHA, it is characterized by different energy eigenvalues, eigenfunctions and re-

duced degeneracies. On the other hand, new degeneracies, namely, *simultaneous, incidental and inter-dimensional degeneracy*, which are non-existent in the free system, is introduced in CHA afresh. Apart from the effect of compression on ground and various energy levels, properties such as dipole shielding factor, nuclear magnetic screening constant, hyper-fine splitting constant, pressure, static and dynamic polarizability, etc., were examined.

An analogous study of compressed He atom is a prototypical non-trivial mathematical problem. Due to the presence of inter-electronic repulsion, the $SU(3)$ symmetry of simplified one-electron case is broken which promises many exciting physics. Ever since the variational calculation of energy variation [23] with respect to cage radius and function of pressure, vigorous attempts have been known. Some of them include Roothaan-HF-type calculation with Slater-type basis [24] or with its modifications [25], configuration interaction [26, 27], quantum Monte Carlo [28], a host of direct variational schemes with appropriate choice of cut-off function [8, 29–31], variational method with B-splines basis [32], Rayleigh-Schrödinger perturbation theory [30, 33]. Some other prominent works are explicitly correlated Hylleraas-type wave functions within variational framework [34–41], a combination of quantum genetic algorithm and HF method [42], variational Monte Carlo [43, 44], HF calculation employing local and global basis sets [45] and so on. Whereas a vast majority of publications have focused on lowest state, low-lying excited states were also treated quite decently. For example, $1sns\ ^1,^3S$ states in [29, 30, 35, 38–42, 44, 46], $1s2p\ ^3P, ^1P$ states in [29, 42, 46], singly excited $1s3d\ ^3D, ^1D$ and some doubly excited states in [42, 46] etc., using a host of theoretical approaches giving results of varied accuracy.

All the above works pertain to the wave function-based methods. In the past two decades, some results have been published within the alternative density-based concept—the so-called density functional theory (DFT) [47–49]. Thus within an exchange-only framework (using two exchange functionals, *viz.*, local density approximation (LDA) [47], and Becke-88 exchange potential [50]), the desired Kohn-Sham (KS) equation was solved satisfying the Dirichlet boundary condition for many-electron systems via numerical shooting method [51]. The usefulness of a one-parameter hybrid exchange functional (including a fraction of exact exchange and Perdew-Burke-Ernzerhof functional) for treatment of confined atoms, has been presented lately [52]. In another attempt, ground and $1s2s\ ^3S, ^1S$ states of confined He atom were reported [53] taking into account the LDA-approximated exchange-correlation (XC) (with Perdew-Wang parametrization for correlation [54]) with and without self-interaction

correction. Response properties such as polarizability and hyperpolarizability of confined He atom were reported within a DFT-based variation-perturbation approach [55]. In a recent work [56], spherically confined atoms were treated by means of local exchange potential corresponding to Zhao-Morrison-Parr and Becke-Johnson potential. Moreover, spherical confinement was used in the comparative study (taking free-ion limit as reference) of behavior of spin potential and pairing energy of first row transition metal cations within KS model [57]. A detailed analysis of correlation energy, performance of several commonly used functionals, electron density as well as the XC potential in some constrained atoms, has been reported [58, 59]. The calculation of static polarizability of confined He and Ne atoms was done through time-dependent DFT in [60].

Recently there has been a growing interest in information theoretical analysis of diverse model and realistic systems. They have found wide-spread applications in many branches of physics and chemistry, such as thermodynamics, spectroscopy, quantum mechanics. In chemical physics, typically they can provide valuable information regarding localization-delocalization, diffusion of atomic orbital, periodic properties, spreading of electron density, correlation energy, etc. Entropic uncertainty measures based on these quantities are arguably the most effective quantifiers of uncertainty, as they do not relate to any specific points of the respective Hilbert space. The present work is particularly concerned with Shannon entropy (S) [61, 62], which is the arithmetic mean of uncertainty. Interestingly S like some of the other measures such as, Fisher information, Onicescu energy and Rényi entropy are functionals of density, and also characterize density. Many articles have been published to analyze these measures in *free* systems (e.g., for free He, we refer the reader to a recent article [63]), but in *confined* quantum systems as treated here, analogous studies are quite limited. Two such reports [64, 65] in CHA are available so far. A systematic variation of S with respect to r_c , in r and p spaces has been presented only lately [66, 67] for $\ell = 0$ as well as non-zero- ℓ states. One finds that, confinement affects S more profoundly in the stronger regime. Further, S_r increases with rise in r_c and at very low- r_c region (≈ 0.1), CHA displays exactly opposite trend from a free H atom (S_r declines with rise in n keeping l fixed). Usually, the effect of perturbation on higher quantum number states is more pronounced. In confined two-electron isoelectronic series (H^- , He, Li^+ , Be^{2+}), S has been reported for only ground states [64] by means of BLYP calculations.

Some reports [52, 68–73] are available on S in *penetrable* confinement in atoms. For

example, it was observed [68] that, in CHA, up to a certain value of r_c , S_r decreases with r_c . However, for small r_c and depending on barrier height, S_r may also increase. Apart from constant potential, it was probed [73] for confinements imposed by a dielectric continuum and by isotropic harmonic potential. It was also proposed [72] as an indicator to measure the delocalization of electron density. Ground-state atomic S 's, as function of width of confining potential was calculated by employing the correlated Hylleraas-type wave function in both repulsive and attractive finite potentials [70]. Confinement by an inert geometric planar boundary with finite barrier height has been studied [69] within a Thomas-Fermi-Dirac-Weizsäcker-type DFT framework. Some limited works exist on excited states as well, *viz.*, low-lying singly [70] and doubly [71] excited states. It is worth noting that, S values in He are available [74] in selected excited states, such as $1,3S^e$, $1,3P^o$ and $1,3D^e$.

The objective of this work is to make a thorough systematic analysis of S in a He-like ion placed inside a spherical cage of radius r_c . This is done by invoking DFT within a work-function-based exchange potential in conjunction with two correlation functionals, *viz.*, a local, parametrized Wigner-type [75] and somewhat involved nonlinear Lee-Yang-Parr (LYP) [76] functional. The pertinent KS differential equation is solved within the Dirichlet boundary condition by means of GPS method in an accurate efficient manner. The electron density as well as S_r is calculated from the self-consistent orbitals. The p -space orbitals are constructed from respective r -space orbitals via standard Fourier transform, from which the S_p 's are computed. Variation of S_r, S_p and total Shannon entropy sum ($S = S_r + S_p$) with respect to r_c is offered for He, Li^+ , Be^{2+} . Apart from ground state, we also consider singly excited $^3S, ^3P, ^3D$ states arising out of configurations $1sns$ ($n = 2-4$) $^3S, 1snp$ ($n = 2-3$) 3P and $1snd$ ($n = 3$). As apparent from the preceding discussion, there is a lack of such results in literature, especially in excited states, and we attempt to provide them. The article is organized as follows. Section II outlines the methodology used, Sec. III discusses the results along with comparison with available references, while Sec. IV makes a few concluding remarks.

II. METHODOLOGY

Here we briefly outline the proposed density functional method for ground and excited states of an arbitrary atom centered inside an impenetrable spherical cavity, followed by the

GPS method for calculation of eigenvalues and eigenenergies of corresponding KS equation. It may be noted that the present method has been very successfully used for ground and various excited states (such as singly, doubly, triply excited states corresponding to low- and high-lying excitation, valence and core excitation, autoionizing states, hollow and doubly hollow states, very high-lying Rydberg states, satellites states etc.) of *free or unconfined* neutral atoms as well as positive and negative ions in a series of articles [77–83]. But it has never been tested for any *confinement* studies as intended here. Thus we present an extension of the method for the purpose of confinement effects. Our focus remains on essential portions, omitting the relevant details, which could be found in above references.

The starting point is the non-relativistic single-particle time-independent KS equation with imposed confinement, which can be conveniently written as (atomic unit employed unless otherwise mentioned),

$$\mathbf{H}(\mathbf{r})\phi_i(\mathbf{r}) = \epsilon_i(\mathbf{r})\phi_i(\mathbf{r}), \quad (1)$$

where \mathbf{H} is the perturbed KS Hamiltonian, written as,

$$\begin{aligned} \mathbf{H}(\mathbf{r}) &= -\frac{1}{2}\nabla^2 + v_{eff}(\mathbf{r}) \\ v_{eff}(\mathbf{r}) &= v_{ne}(\mathbf{r}) + \int \frac{\rho(\mathbf{r}')}{|\mathbf{r} - \mathbf{r}'|} d\mathbf{r}' + \frac{\delta E_{xc}[\rho(\mathbf{r})]}{\delta \rho(\mathbf{r})} + v_{conf}(\mathbf{r}). \end{aligned} \quad (2)$$

In the above, $v_{ne}(\mathbf{r})$ and $v_{conf}(\mathbf{r})$ signify external electron-nuclear attraction and the effective confining potentials, whereas second and third terms in right-hand side denote classical Coulomb (Hartree) repulsion and many-body XC potentials respectively. The desired confinement effect is built into the system by introducing a potential of following form (r_c refers to the radius of spherical enclosure),

$$v_{conf}(\mathbf{r}) = \begin{cases} 0, & r \leq r_c \\ +\infty, & r > r_c. \end{cases} \quad (3)$$

Though DFT has achieved impressive success in explaining the electronic structure and properties of many-electron system in ground state in past four decades, calculation of excited-state energies and densities has remained a bottleneck. This is mainly due to the absence of a Hohenberg-Kohn theorem parallel to ground state, as well as the lack of a suitable XC functional valid for a general excited state. In this work, we have employed an accurate work-function-based exchange potential, which is physically motivated [84, 85].

Accordingly, exchange energy is interpreted as the interaction energy between an electron at \mathbf{r} and its Fermi-Coulomb hole charge density $\rho_x(\mathbf{r}, \mathbf{r}')$ at \mathbf{r}' , and given by,

$$E_x[\rho(\mathbf{r})] = \frac{1}{2} \int \int \frac{\rho(\mathbf{r})\rho_x(\mathbf{r}, \mathbf{r}')}{|\mathbf{r} - \mathbf{r}'|} d\mathbf{r} d\mathbf{r}'. \quad (4)$$

Assuming that a unique local exchange potential $v_x(\mathbf{r})$ exists for a given state, it can be defined as the work done in bringing an electron to the point \mathbf{r} against the electric field generated by its Fermi-Coulomb hole density, leading to the following form,

$$v_x(\mathbf{r}) = - \int_{\infty}^{\mathbf{r}} \mathcal{E}_x(\mathbf{r}) d\mathbf{l}, \quad (5)$$

where the electric field is expressed as,

$$\mathcal{E}_x(\mathbf{r}) = \int \frac{\rho_x(\mathbf{r}, \mathbf{r}')(\mathbf{r} - \mathbf{r}')}{|\mathbf{r} - \mathbf{r}'|^3} d\mathbf{r}'. \quad (6)$$

The Fermi hole can be written in terms of orbitals as,

$$\rho_x(\mathbf{r}, \mathbf{r}') = - \frac{|\gamma(\mathbf{r}, \mathbf{r}')|^2}{2\rho(\mathbf{r})}, \quad (7)$$

where $|\gamma(\mathbf{r}, \mathbf{r}')| = \sum_i \phi_i^*(\mathbf{r})\phi_i(\mathbf{r}')$ is the single-particle density matrix and $\rho(\mathbf{r})$ is the electron density, expressed in terms of occupied atomic orbitals (n_i denotes occupation number) as,

$$\rho(\mathbf{r}) = \sum_{i=1}^N n_i |\phi_i(\mathbf{r})|^2. \quad (8)$$

While the exchange potential $v_x(\mathbf{r})$ corresponding to a given state arising from an electronic configuration can be accurately calculated by the above procedure as delineated, the correlation potential $v_c(\mathbf{r})$ is unknown and must be approximated for practical calculations. The current work incorporates two correlation functionals, namely, a Wigner-type [75] and LYP [76]. These two functionals have been chosen on the basis of their success in the *unconfined* atomic excited states, which are recorded in the references [77–83]. This work will help shed some light on the applicability of such functionals in the context of *confined* quantum systems, including those studied here.

With this choice of $v_x(\mathbf{r})$ and $v_c(\mathbf{r})$, the resulting KS differential equation,

$$\left[-\frac{1}{2}\nabla^2 + v_{eff}(\mathbf{r}) \right] \phi_i(\mathbf{r}) = \varepsilon_i \phi_i(\mathbf{r}), \quad (9)$$

needs to be solved, where $v_{eff}(\mathbf{r})$ is as defined in Eq. (2), maintaining the Dirichlet boundary condition. For an accurate and efficient solution, we have adopted GPS scheme leading

to a non-uniform, optimal spatial discretization. It is simple but very effective method; the success has been demonstrated for many static and dynamic properties of a variety of *singular* and non-singular potentials of physical and chemical interest [80–83, 86–89] such as, Coulomb, Hülthen, Yukawa, logarithmic, spiked oscillator, Hellmann potential, etc., along with its recent extension to quantum confinement [15, 21, 22]. As the method is very well established and documented, in the following, we will mention a very brief summary of it; the details are available in the cited references.

The key characteristic of this approach is to approximate an *exact* function $f(x)$ defined in the interval $[-1, 1]$ by an N th-order polynomial $f_N(x)$,

$$f(x) \cong f_N(x) = \sum_{j=0}^N f(x_j)g_j(x), \quad (10)$$

which ensures that the approximation be *exact* at the *collocation points* x_j ,

$$f_N(x_j) = f(x_j). \quad (11)$$

Here we utilize the Legendre pseudo-spectral method where $x_0 = -1$, $x_N = 1$, while x_j ($j = 1, \dots, N - 1$)'s are defined by roots of first derivative of Legendre polynomial $P_N(x)$, with respect to x , namely,

$$P'_N(x_j) = 0. \quad (12)$$

In Eq. (10), $g_j(x)$ are termed *cardinal functions*, and as such, expressed as,

$$g_j(x) = -\frac{1}{N(N+1)P_N(x_j)} \frac{(1-x^2)P'_N(x)}{(x-x_j)}, \quad (13)$$

fulfilling the unique property that, $g_j(x_{j'}) = \delta_{j',j}$. Then use of a non-linear mapping followed by a symmetrization procedure, eventually leads to a symmetric eigenvalue problem, which is solved by standard available softwares to provide accurate eigenvalues and eigenfunctions.

The p -space wave function is obtained numerically from Fourier transform of respective r -space counterpart in the following way,

$$\xi(\mathbf{p}) = \left(\frac{1}{2\pi}\right)^{3/2} \int \phi(\mathbf{r}) e^{i\mathbf{p}\cdot\mathbf{r}} d\mathbf{r}. \quad (14)$$

It is to be noted here that $\xi(\mathbf{p})$ is not normalized; hence needs to be normalized. The normalized r - and p -space densities are represented as $\rho(\mathbf{r}) = \sum_{i=1}^N n_i |\phi_i(\mathbf{r})|^2$ and $\Pi(\mathbf{p}) = \sum_{i=1}^N n_i |\xi_i(\mathbf{p})|^2$ respectively, where n_i represents the occupation number of each orbital.

Next $S_{\mathbf{r}}$, $S_{\mathbf{p}}$ and Shannon entropy sum S_t are defined in terms of expectation values of logarithmic probability density functions, which have the forms given below as,

$$S_{\mathbf{r}} = - \int_{\mathcal{R}^3} \rho(\mathbf{r}) \ln[\rho(\mathbf{r})] d\mathbf{r}, \quad S_{\mathbf{p}} = - \int_{\mathcal{R}^3} \Pi(\mathbf{p}) \ln[\Pi(\mathbf{p})] d\mathbf{p}, \quad (15)$$

$$S_t = [S_{\mathbf{r}} + S_{\mathbf{p}}] \geq 3(1 + \ln \pi), \quad \text{in 3 dimension.}$$

Here $\rho(\mathbf{r})$ and $\Pi(\mathbf{p})$ are both normalized to unity.

All the computations are done numerically. The convergence is ensured by carrying out calculations with respect to variation in grid parameters, such as total number of radial points and maximum range of grid. It is generally observed that convergence is achieved relatively easily in the lower r_c region compared to the $r_c \rightarrow \infty$ limit. All results given in the following tables and plots have been checked for above convergence.

III. RESULT AND DISCUSSION

At the onset, it would be appropriate to mention a few points to facilitate the discussion. The net information measures in r and p space of confined many-electron system consist of (i) radial and (ii) angular contributions. The angular part remains invariant in both spaces with respect to change in boundary condition resulting from confinement. Note that, an analogous energy analysis with respect to r_c in these and other excited states, would be presented elsewhere. However, it suffices here to mention that, energies for both ground and excited states obtained with the present method are in good agreement with those available in literature. Here our aim is to investigate S for confined two-electron atomic systems at various r_c in several low-lying states. These are calculated for spherically confined He and extended to confined iso-electronic members, namely, Li^+ and Be^{2+} . Apart from ground state, following low-lying singly excited states have been considered, *viz.*, $1sns \ ^3S$ with $n=2-4$; $1snp \ ^3P$ with $n=2-3$; $1snd \ ^3D$ having $n=3$. The necessary results are presented in the following tables and plots along with available literature values, for a comparative discussion. All calculations are performed with unit-normalized density.

To start with, Table I imprints the numerical results of $S_{\mathbf{r}}$, $S_{\mathbf{p}}$, S_t for confined He, Li^+ and Be^{2+} in their ground states. In order to put things in perspective, here and in all other tables, three sets of calculations have been performed at each r_c , namely, (i) exchange-only (ii) XC with Wigner correlation (iii) XC with LYP correlation. Throughout the article, these three

TABLE I: $S_{\mathbf{r}}, S_{\mathbf{p}}, S_t$ (a.u.) in ground states of confined He, Li⁺, Be²⁺. See text for details.

Species	r_c	X-only			XC-Wigner			XC-LYP			Literature ^a		
		$S_{\mathbf{r}}$	$S_{\mathbf{p}}$	S_t	$S_{\mathbf{r}}$	$S_{\mathbf{p}}$	S_t	$S_{\mathbf{r}}$	$S_{\mathbf{p}}$	S_t	$S_{\mathbf{r}}$	$S_{\mathbf{p}}$	S_t
He ^{b,c}	0.1	-6.2534	12.855	6.5744	-6.2534	12.855	6.5744	-6.2534	12.855	6.5744			
	0.3	-3.004	9.580	6.576	-3.004	9.580	6.576	-3.004	9.580	6.576	-2.988	9.488	6.5
	0.5	-1.525	8.075	6.550	-1.525	8.075	6.550	-1.525	8.075	6.550	-1.498	8.023	6.525
	1	0.389	6.118	6.507	0.387	6.119	6.506	0.388	6.118	6.506	0.4326	6.078	6.51
	1.4	1.22	5.273	6.493	1.22	5.276	6.49	1.22	5.327	6.547	1.2739	5.234	6.508
	2	1.97	4.547	6.517	1.96	4.555	6.515	1.96	4.549	6.509	2.0097	4.519	6.528
	3	2.50	4.061	6.561	2.48	4.080	6.560	2.50	4.068	6.568	2.5241	4.057	6.581
	4	2.65	3.943	6.593	2.63	3.969	6.599	2.64	3.952	6.592	2.6651	3.945	6.61
	5	2.68	3.921	6.608	2.65	3.95	6.60	2.67	3.932	6.602	2.7042	3.918	6.622
6	2.69	3.918	6.608	2.66	3.95	6.61	2.68	3.93	6.61	2.7106	3.914	6.625	
7	2.69	3.918	6.608	2.66	3.95	6.61	2.68	3.93	6.61	2.7117	3.913	6.625	
Li ^{+d,e}	0.1	-6.2665	12.860	6.5935	-6.2665	12.860	6.5935	-6.2665	12.860	6.5935			
	0.3	-3.050	9.604	6.554	-3.050	9.604	6.554	-3.050	9.604	6.554	-3.034	9.538	6.504
	0.8	-0.392	6.890	6.498	-0.393	6.891	6.498	-0.392	6.890	6.498	-0.353	6.849	6.496
	1	0.12	6.376	6.496	0.121	6.378	6.499	0.122	6.377	6.499	0.1659	6.335	6.501
	2	1.135	5.431	6.566	1.12	5.440	6.56	1.13	5.43	6.56	1.174	5.4	6.574
	2.5	1.22	5.361	6.581	1.21	5.373	6.58	1.22	5.36	6.58	1.2618	5.331	6.593
	3	1.24	5.346	6.586	1.23	5.358	6.58	1.24	5.34	6.58	1.2878	5.313	6.601
	4	1.25	5.343	6.593	1.23	5.355	6.58	1.24	5.34	6.58	1.2942	5.309	6.603
7	1.25	5.343	6.593	1.23	5.355	6.58	1.24	5.34	6.58				
Be ²⁺	0.1	-6.2801	12.866	6.5859	-6.2801	12.866	6.5859	-6.2801	12.866	6.5859			
	0.3	-3.102	9.636	6.534	-3.102	9.636	6.534	-3.102	9.636	6.534			
	0.5	-1.725	8.226	6.501	-1.725	8.226	6.501	-1.725	8.226	6.501			
	1	-0.229	6.748	6.519	-0.231	6.750	6.519	-0.229	6.748	6.519			
	1.5	0.191	6.373	6.564	0.186	6.378	6.564	0.190	6.374	6.564			
	2	0.27	6.311	6.581	0.26	6.317	6.577	0.26	6.312	6.572			
	2.5	0.28	6.305	6.585	0.27	6.311	6.581	0.26	6.306	6.566			
	3	0.28	6.305	6.585	0.27	6.311	6.581	0.26	6.306	6.566			
7	0.28	6.305	6.585	0.27	6.311	6.581	0.26	6.306	6.566				

^aDFT calculation [64], using BLYP functional.

^bFor free atom, using N -normalized HF density— $S_{\mathbf{r}}$: 4.01 [72], 4.06 [90], 4.0100 [91], 4.0107 [52]; $S_{\mathbf{p}}$: 6.45 [90]; S_t : 10.52 [90].

Our X-only results are 4.00, 6.45 and 10.52 respectively.

^cCorrelated $S_{\mathbf{r}}$ values in free He atom: (i) unit-normalized density: 2.7051028 [92], 2.705 [93] (ii) N-normalized density: 4.40106, (Variational Monte Carlo), 4.0256 (Diffusion Monte Carlo) [91]. Our XC results are 3.93 (XC-Wigner) and 3.96 (XC-LYP).

^dHF $S_{\mathbf{r}}$ value in free Li⁺ ion using N-normalized density: 1.1023 [91]. Our X-only result is 1.11.

^eCorrelated $S_{\mathbf{r}}$ value in Li⁺ ion: (i) unit-normalized density: 1.2552726 [92] (ii) N-normalized density: 1.1204 (Variational Monte Carlo), [91]. 1.1143 (Diffusion Monte Carlo). Our XC results are: 1.08 (XC-Wigner), 1.10 (XC-LYP).

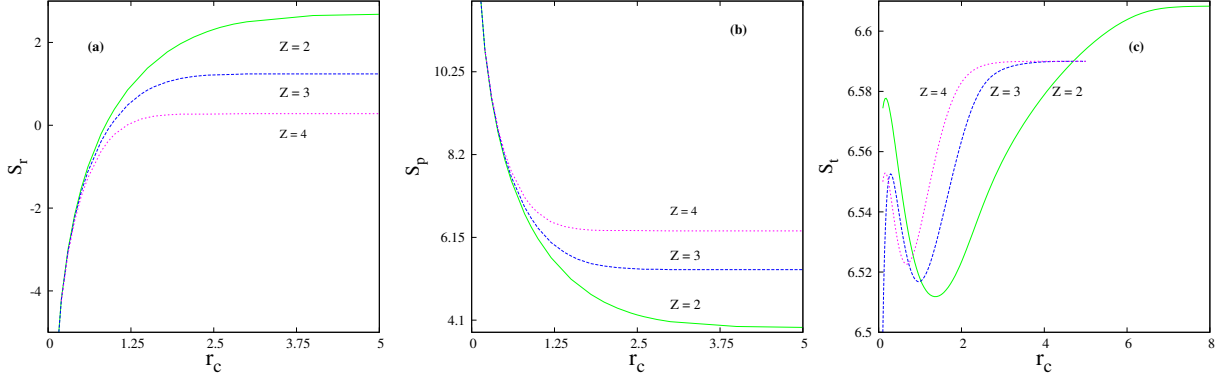


FIG. 1: Variation of S_r, S_p, S_t for He-isoelectronic series ($Z = 2 - 4$) with r_c in panels (a)–(c).

results are denoted by labels X-only, XC-Wigner and XC-LYP respectively. This can give us an idea how X-only and HF results compare and contrast. Moreover, it will help us in getting a sense of correlation contribution in current context, approximated by two functionals. In all three occasions (i)–(iii), S_r 's increase with rise in r_c and finally merge to corresponding free atom entropy at a sufficiently large r_c . The reported values of S_r in this table further reinforces the previous conclusions [64, 72] that impenetrable walls impose confinements in a way that localizes the electron density, and consequently $S_r \rightarrow -\infty$ when $r_c \rightarrow 0$. However, it is important to point out that, in all these cases total energy monotonically decreases with r_c eventually reaching the free-atom limit. Actually, with reduction in r_c the r -space electron density gets compressed and as a consequence, S_r decreases. On the contrary, S_p gradually abates with progress in r_c . At all r_c 's, however, S_t maintains the lower bound (6.434) governed by the well-known BBM inequality [62]. The qualitative behavior of S_r, S_p, S_t with growth in r_c does not change much with atomic charge (Z), although their numerical values differ. In fact, at a given r_c , S_r regresses and S_p progresses with advancement of Z . With rise in Z , electron density gets compressed and hence such a pattern is noticed. Interestingly, while in one-electron systems S_t does not depend on Z , in a many-electron atom, with change of Z it varies [94]. Earlier S_t has been mentioned as a measure of correlation in free systems. Our work establishes the same fact in confinement as well. It is noticed that, for all the three species, S 's are identical at very low r_c region (≤ 0.5), *without or with* (either Wigner or LYP) correlation. Furthermore, these two results begin to differ at larger r_c indicating correlation effects to assume more significance in the respective *free-atom* case. In other words, this implies that, at smaller r_c region, XC effect is minimum, which enhances with rise in r_c . Similar conclusions have been found in the energy analysis

of confined He in [55]. For He and Li^+ , these have been estimated by BLYP calculation [64] in most of the r_c 's considered here, which are appropriately quoted. Note that the HF values [90] for $S_{\mathbf{r}}, S_{\mathbf{p}}, S_t$ in ground state of unconfined He match reasonably well with our X-only results. Since we are unable to find reference theoretical results for X-only S 's in the *hard* confinement, for direct comparison, as a matter of check, a couple of comparisons on respective *free* systems is provided here. Thus the literature $S_{\mathbf{r}}, S_{\mathbf{p}}, S_t$ values of He and Li^+ within HF method [90, 91], employing N -normalized densities, given in footnote of the table, are in reasonable agreement with our X-only values. Recently, in a *penetrable* confinement calculation within HF, some results on $S_{\mathbf{r}}$ have been presented [72]. The same has also been calculated from a DFT-based study with hybrid exchange functional [52]. Results for He in *free*-limit from both these studies, presented in footnote show quite decent agreement with ours. It may be noted that in these two aforementioned references $S_{\mathbf{r}}$ in $U_0 \rightarrow \infty$ corresponds to the impenetrable confinement. Highly accurate benchmark-quality result for $S_{\mathbf{r}}$ was calculated from a Hylleraas-type variational method producing a value of 2.7051028 and 1.2552726 for free He and Li^+ [92] respectively. Correlated results obtained from variational Monte carlo and diffusion Monte Carlo methods [91] for He and Li^+ are also cited in the footnote. The current single-determinantal approach quite nicely compares with reference values in the table–XC-LYP providing a slight edge over XC-Wigner. It would be worthwhile to make a comparative energy analysis of these two functionals, which we intend to do in near future. No reference entropies are available for Be^{2+} .

A careful examination of Table I reveals that, X-only, XC-Wigner and XC-LYP results provide similar qualitative trend with respect to changes in r_c , for all three species. Hence in Fig. 1, X-only $S_{\mathbf{r}}, S_{\mathbf{p}}$ and S_t are plotted for ground state of all three isoelectronic members, as functions of r_c in panels (a)–(c). The first two panels imply that, for a fixed Z , $S_{\mathbf{r}}, S_{\mathbf{p}}$ go up and down respectively with rise in r_c . On the contrary, for a given r_c , variation of these two quantities with Z shows opposite trend; the former decays and latter develops as Z advances. These results reinforce the inferences drawn from Table I. Another point to be noted here is that, with lowering in r_c the difference between $S_{\mathbf{r}}$ and $S_{\mathbf{p}}$ corresponding to two successive members of the isoelectronic series, diminishes; in other words, as r_c enhances, so does the difference. As r_c declines, both average electron-nucleus and electron-electron distances fall down. In stronger confinement regime, the effect of Z on ground state gets dominated by confining potential, resulting in the fact that the three $S_{\mathbf{r}}, S_{\mathbf{p}}$ plots very nearly

TABLE II: S_r, S_p, S_t (a.u.) in $1s2s\ ^3S$ states of confined He, Li^+ , Be^{2+} . See text for details.

Species	r_c	X-only			XC-Wigner			XC-LYP		
		S_r	S_p	S_t	S_r	S_p	S_t	S_r	S_p	S_t
He ^a	0.1	-6.2172	14.190	7.9728	-6.2172	14.190	7.9728	-6.2172	14.190	7.9728
	0.5	-1.4472	9.376	7.9288	-1.4472	9.376	7.9288	-1.4472	9.3756	7.9288
	1	0.547	7.333	7.880	0.547	7.333	7.880	0.547	7.333	7.880
	2	2.417	5.409	7.826	2.415	5.410	7.825	2.417	5.409	7.826
	4	3.956	3.86	7.819	3.948	3.87	7.818	3.953	3.86	7.813
	6	4.60	3.22	7.82	4.59	3.23	7.82	4.59	3.23	7.82
	6.5	4.71	3.11	7.82	4.69	3.13	7.82	4.69	3.13	7.82
	7.5	4.87	2.94	7.81	4.85	2.96	7.81	4.85	2.97	7.82
	8.5	4.99	2.81	7.80	4.96	2.84	7.80	4.96	2.85	7.81
	10	5.10	2.69	7.79	5.06	2.72	7.78	5.03	2.75	7.78
Li ⁺	0.1	-6.2246	14.191	7.9664	-6.2246	14.191	7.9664	-6.2246	14.191	7.9664
	0.5	-1.4905	9.392	7.9015	-1.4905	9.392	7.9015	-1.4905	9.392	7.9015
	1	0.442	7.401	7.843	0.442	7.401	7.843	0.442	7.401	7.843
	1.5	1.481	6.335	7.816	1.480	6.336	7.816	1.481	6.336	7.817
	2	2.141	5.669	7.810	2.138	5.671	7.809	2.140	5.669	7.809
	3	2.910	4.90	7.810	2.905	4.90	7.805	2.909	4.905	7.814
	4	3.32	4.49	7.81	3.312	4.49	7.802	3.31	4.49	7.80
	7	3.70	4.07	7.77	3.68	4.09	7.77	3.69	4.09	7.78
	8.5	3.72	4.05	7.77	3.70	4.07	7.77	3.70	4.07	7.77
	10	3.72	4.05	7.77	3.70	4.07	7.77	3.70	4.07	7.77
Be ²⁺	0.1	-6.2320	14.191	7.9590	-6.2320	14.191	7.9590	-6.2320	14.191	7.9590
	0.5	-1.5376	9.415	7.8774	-1.537	9.415	7.8774	-1.5376	9.415	7.8774
	1	0.322	7.499	7.821	0.322	7.500	7.822	0.322	7.499	7.821
	2	1.829	5.981	7.810	1.826	5.983	7.809	1.828	5.981	7.809
	3	2.42	5.38	7.80	2.141	5.39	7.531	2.418	5.38	7.798
	4	2.66	5.12	7.78	2.651	5.13	7.781	2.656	5.12	7.776
	5	2.73	5.03	7.76	2.72	5.05	7.77	2.72	5.04	7.76
	6	2.75	5.02	7.77	2.73	5.03	7.76	2.74	5.02	7.76
	20	2.75	5.02	7.77	2.73	5.03	7.76	2.74	5.02	7.76

^aCorrelated S_r value in free atom is: 5.239 [93].

coincide. For a fixed Z , variation of S_t with r_c in panel (c) suggests that the entropy sum reduces dramatically from its free atomic value as r_c is lowered. With enhanced confinement, a distinct minimum followed by a maximum shows up in the curve for all He-like ions. The minimum tends to shift towards left as Z progresses. This observed pattern is in consonance with that found in [64].

Now we move on to some low-lying singly excited state- S_r, S_p, S_t for He, Li^+ and Be^{2+}

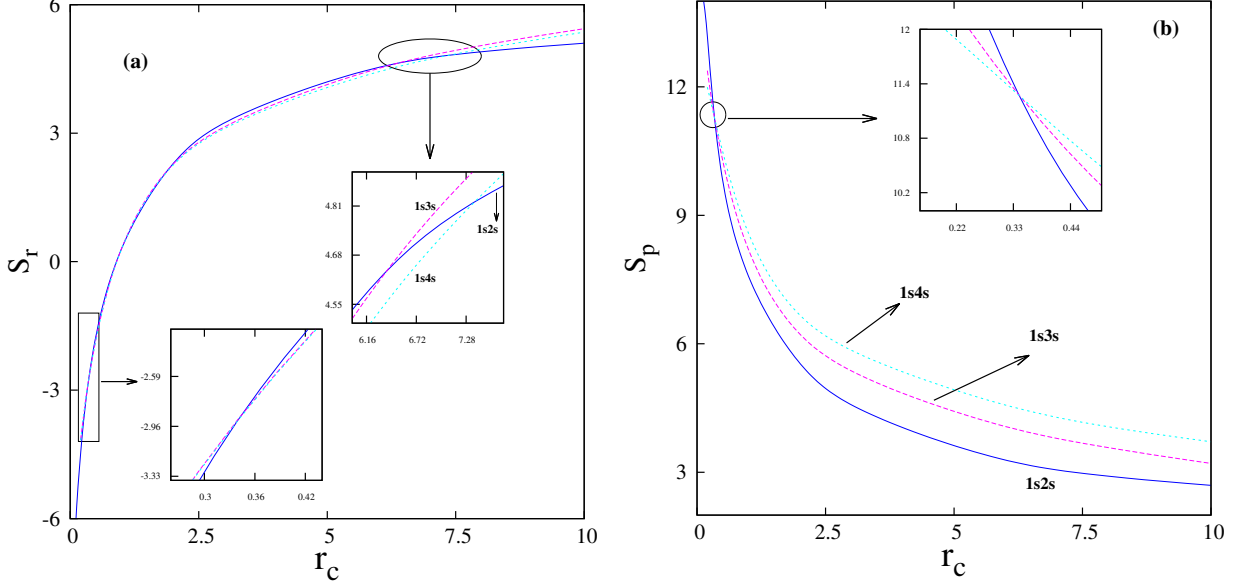


FIG. 2: Variation of S_r , S_p in $1sns$ 3S ($n = 2-4$) states of confined He with r_c . See text for details.

in Tables II-IV. Following the presentation strategy of previous table, it reports results for $1s2s$ 3S , $1s2p$ 3P and $1s3d$ 3D states respectively. Like the ground state, here also in all three states, both X-only and correlation-included S_r , S_p moves up and down respectively with growth in r_c . In all cases again S_t obeys the stipulated lower bound [62]. The qualitative pattern of S_r , S_p , S_t with progress in r_c remains invariant with change of Z . However, their numerical values alter substantially. Similar to the ground state, at a fixed r_c , S_r falls off and S_p enhances with advancement of Z . Once again, for a given Z , at low r_c region, X-only, XC-Wigner and XC-LYP results practically merge with each other, signifying that the effect of correlation is somewhat less impactful in stronger confinement region, as the confining potential leads the contribution in this scenario. Whereas, with rise in r_c , the correlation effect prevails, indicating its importance in *free* conditions. Except the free atom-limit of S_r in $1s2s$ 3S He, no reference results could be found for any of the confined states and we hope the present work would provide useful guideline in future.

In order to gain a better understand of the effect of confinement on excited states, S_r , S_p in compressed He have been plotted in panels (a), (b) of Fig. 2, for three triplet singly excited states arising from configuration $1sns$, corresponding to $n = 2-4$. Since correlation does not affect the results qualitatively, for this purpose, it suffices to consider X-only results. With this in mind, here and in next figure, only X-only entropies are shown. It is obvious from these plots that, for excited states, as in Fig. 1, S_r gains with rise in r_c , while S_p

TABLE III: S_r, S_p, S_t (a.u.) in $1s2p\ ^3P$ states of confined He, Li^+ , Be^{2+} . See text for details.

Species	r_c	X-only			XC-Wigner			XC-LYP		
		S_r	S_p	S_t	S_r	S_p	S_t	S_r	S_p	S_t
He ^a	0.5	-1.392	8.596	7.204	-1.392	8.596	7.204	-1.392	8.596	7.204
	0.8	-0.031	7.213	7.182	-0.031	7.213	7.182	-0.031	7.213	7.182
	1	0.60	6.570	7.170	0.60	6.570	7.170	0.60	6.570	7.170
	3	3.26	4.04	7.30	3.26	4.05	7.31	3.26	4.04	7.30
	5	4.09	3.49	7.58	4.08	3.50	7.58	4.08	3.50	7.58
	6	4.35	3.34	7.69	4.32	3.36	7.68	4.33	3.35	7.68
	7	4.54	3.23	7.77	4.51	3.25	7.76	4.51	3.25	7.76
	7.6	4.63	3.18	7.81	4.58	3.21	7.79	4.58	3.21	7.79
	8	4.68	3.15	7.83	4.65	3.18	7.83	4.64	3.18	7.82
	10	4.86	3.04	7.90	4.82	3.08	7.90	4.78	3.10	7.88
Li ⁺	0.5	-1.437	8.620	7.183	-1.437	8.620	7.183	-1.437	8.620	7.183
	0.8	-0.121	7.284	7.163	-0.121	7.284	7.163	-0.121	7.284	7.163
	1	0.471	6.693	7.164	0.470	6.694	7.164	0.47	6.69	7.16
	1.5	1.44	5.91	7.35	1.438	5.91	7.358	1.44	5.91	7.35
	2	2.009	5.29	7.299	2.005	5.30	7.305	2.008	5.30	7.308
	3	2.65	4.85	7.50	2.64	4.86	7.50	2.653	4.86	7.513
	6	3.33	4.47	7.80	3.31	4.49	7.80	3.31	4.48	7.79
	8	3.39	4.45	7.84	3.36	4.47	7.83	3.37	4.47	7.84
	9	3.40	4.45	7.85	3.36	4.47	7.83	3.37	4.47	7.84
	10	3.40	4.45	7.85	3.37	4.47	7.84	3.37	4.47	7.84
Be ²⁺	0.5	-1.490	8.658	7.168	-1.490	8.658	7.168	-1.490	8.658	7.168
	0.8	-0.235	7.402	7.167	-0.235	7.402	7.167	-0.235	7.402	7.167
	1.2	0.698	6.532	7.23	0.697	6.534	7.231	0.698	6.532	7.23
	2	1.589	5.857	7.446	1.585	5.861	7.446	1.588	5.858	7.446
	2.5	1.892	5.670	7.562	1.88	5.67	7.55	1.890	5.701	7.591
	5	2.37	5.41	7.78	2.35	5.43	7.78	2.36	5.42	7.78
	6	2.38	5.41	7.79	2.36	5.42	7.78	2.37	5.42	7.79
	10	2.38	5.41	7.79	2.36	5.42	7.78	2.37	5.42	7.79

^aCorrelated S_r value in free atom is: 5.356. [74].

declines. Now for a fixed r_c , the behavior of S_r with n (in this series), shows interesting pattern. For a large enough value of r_c , which corresponds to the free-atom limit of He of the state under consideration, S_r progresses as n grows. Though it may not be so apparent from the data presented in respective table or plot, as the maximum range of r_c presented here is 10 a.u. This can be concluded from the fact that S_r for $1s2s$, $1s3s$ and $1s4s$ triplet states in the free limit are 5.20, 6.53, 7.43 respectively, signifying a progressive delocalization. But this pattern gets dissolved with reduction in r_c and crossing between S_r for different

TABLE IV: S_r, S_p, S_t (a.u.) in $1s3d$ 3D states of confined He, Li^+ , Be^{2+} . See text for details.

Species	r_c	X-only			XC-Wigner			XC-LYP		
		S_r	S_p	S_t	S_r	S_p	S_t	S_r	S_p	S_t
He ^a	0.5	-1.3053	9.110	7.8047	-1.3053	9.110	7.8047	-1.3053	9.110	7.8047
	1	0.707	7.073	7.780	0.706	7.073	7.779	0.707	7.073	7.780
	1.5	1.828	5.938	7.766	1.826	5.939	7.765	1.827	5.938	7.765
	2.6	3.155	4.640	7.795	3.150	4.645	7.795	3.153	4.641	7.794
	4	3.960	3.957	7.917	3.951	3.967	7.918	3.957	3.960	7.917
	5	4.327	3.687	8.014	4.317	3.699	8.016	4.323	3.691	8.014
	6	4.61	3.48	8.09	4.60	3.50	8.10	4.60	3.49	8.09
	7	4.85	3.33	8.18	4.83	3.34	8.17	4.83	3.34	8.17
	8	5.04	3.19	8.23	5.03	3.21	8.24	5.02	3.22	8.24
	10	5.36	2.97	8.33	5.35	2.99	8.34	5.27	3.04	8.24
Li ⁺	0.5	-1.339	9.129	7.790	-1.339	9.129	7.790	-1.339	9.129	7.790
	0.8	-0.003	7.774	7.771	-0.003	7.774	7.771	-0.003	7.774	7.771
	1	0.601	7.161	7.762	0.601	7.161	7.762	0.601	7.161	7.762
	2.5	2.611	5.27	7.881	2.608	5.280	7.888	2.611	5.277	7.888
	3	2.918	5.042	7.960	2.914	5.047	7.961	2.917	5.043	7.960
	4	3.373	4.72	8.093	3.36	4.73	8.09	3.37	4.72	8.09
	5	3.704	4.50	8.204	3.69	4.51	8.20	3.70	4.50	8.20
	6.5	4.06	4.26	8.32	4.05	4.27	8.32	4.05	4.27	8.32
	7	4.16	4.20	8.36	4.15	4.21	8.36	4.14	4.21	8.35
	7.5	4.24	4.14	8.38	4.23	4.15	8.38	4.22	4.16	8.38
10	4.53	3.97	8.50	4.51	3.99	8.50	4.46	4.03	8.49	
Be ²⁺	0.5	-1.3803	9.157	7.776	-1.3803	9.157	7.776	-1.3803	9.157	7.776
	0.8	-0.097	7.857	7.760	-0.097	7.857	7.760	-0.097	7.857	7.760
	1	0.460	7.303	7.763	0.459	7.304	7.763	0.460	7.303	7.763
	2.5	2.21	5.79	8.00	2.211	5.79	8.001	2.213	5.79	8.003
	3	2.496	5.59	8.086	2.492	5.60	8.092	2.495	5.59	8.085
	4	2.911	5.32	8.231	2.907	5.32	8.227	2.909	5.32	8.229
	7	3.53	4.94	8.47	3.51	4.96	8.47	3.51	4.96	8.47
	8	3.60	4.91	8.51	3.59	4.92	8.51	3.58	4.93	8.51
	8.5	3.63	4.90	8.53	3.61	4.92	8.53	3.60	4.92	8.52
	10	3.66	4.90	8.62	3.64	4.91	8.55	3.62	4.92	8.54

^aCorrelated S_r value in free atom is: 6.634 [74].

states occurs. From the inset plots of panel (a) it is noticed that, at $r_c \approx 7.43$ there is a crossing between $S_r^{(1s2s)}$ and $S_r^{(1s4s)}$; another crossing occurs at $r_c \approx 6.36$ between $S_r^{(1s3s)}$ and $S_r^{(1s4s)}$. With further gain in confinement strength, at $r_c \approx 0.33$ and 0.34 , crossings take place between $S_r^{(1s2s)}$, $S_r^{(1s4s)}$ and $S_r^{(1s2s)}$, $S_r^{(1s3s)}$ respectively. Hence, one encounters frequent change in the order arrangement on proceeding from free to strong confined regime. In

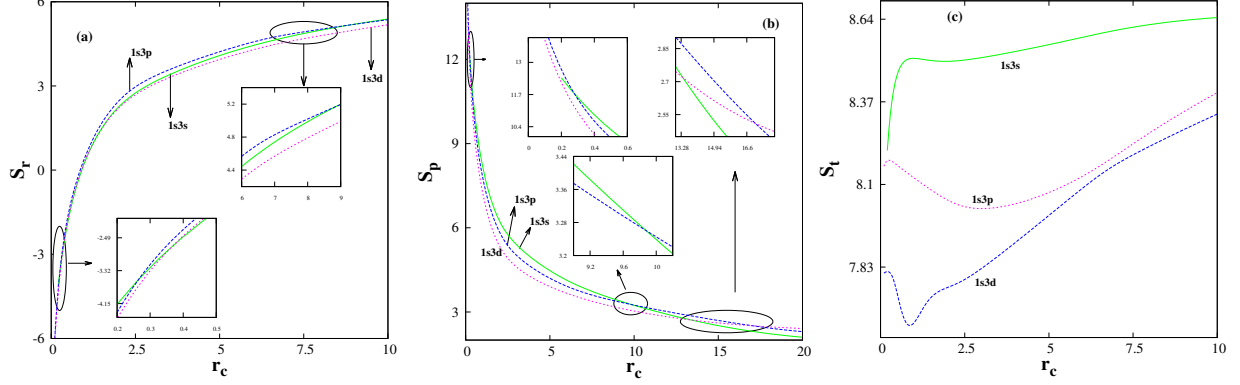


FIG. 3: S_r, S_p, S_t in $1s3s\ ^3S, 1s3p\ ^3P, 1s3d\ ^3D$ states of confined He, against r_c . See text for details.

the strong confinement regime ($r_c \approx 0.1$) the following ordering of entropy holds good: $S_r^{(1s2s)} > S_r^{(1s3s)} > S_r^{(1s4s)}$. Apparently, there exists an interplay between two competing effects, namely, (i) radial confinement (localization) and (ii) accumulation of nodes and humps with growth in n (delocalization). And these two opposing forces control the ordering of S values of these states. Similarly, in p space also, such crossovers prevail at various r_c 's. However, at $r_c \rightarrow \infty$ limit and $r_c = 0.1$, S_p shows opposite trend to that of S_r .

As a continuation of the earlier discussion, we present in Fig. 3, X-only S_r, S_p and S_t as a functions of r_c corresponding to $^3S, ^3P$ and 3D states resulting from $1s3s, 1s3p$ and $1s3d$ configurations of He, in panels (a)–(c). From panel (a), at $r_c \approx 10$, we obtain the following ordering of entropy: $S_r(^3S) > S_r(^3P) > S_r(^3D)$, indicating a drop in fluctuation as one passes from 3S to 3P to 3D . Similar to that in Fig. 2, here also multiple crossovers take place at intermediate and lower r_c region and eventually settles with the following sequential order $S_r(^3P) > S_r(^3S) > S_r(^3D)$ at ($r_c \approx 0.1$), representing strong confinement region. Now in conjugate space, at higher r_c region ≈ 20 , S_p displays an exact opposite trend to that of S_r in the free limit, which is depicted in panel (b). This is obvious as the more localized a state is in r space, the more diffused it is in p space. Here also due to crossover between states this pattern gets dissolved at lower r_c , leading to an ordering as $S_p(^3S) > S_r(^3P) > S_r(^3D)$, at $r_c \approx 0.1$. Panel (c) portrays the response of S_t which verifies that the lower bound is maintained throughout entire confinement region.

IV. CONCLUSION

Shannon information entropy (in r and p spaces) has been analyzed for confined He iso-electronic series. Ground and excited states were studied via a simple DFT method, by solving the radial KS equation through a generalized Legendre pseudospectral method. Some attempts are known for S of *free* He atom, as well as its confinement within a *soft, penetrable* boundary. However to the best of our knowledge, this is the first such systematic study of information in confined two-electron atom within a rigid, impenetrable spherical cage. Apart from ground state, several low-lying singly excited triplet states of the iso-electronic series are considered. As the X-only entropies are comparable to their HF counterparts in the free-atom limit, it is expected that this will also hold in the confined case as well. The effects of electron correlation have been probed through two correlation functionals. For the states considered here, the correlation contribution remains rather small in low r_c regime, assuming greater significance as the latter approaches free-atom limit. It is observed that the two correlation functionals offer quite comparable results as far as Shannon entropy is concerned. To get more accurate results, it would be necessary to design/employ proper correlation functionals suited for confined systems.

It is seen that S_r amplifies and S_p declines with rise in r_c , in both ground and excited states under consideration. Besides, for a particular confinement strength, as Z grows, the state of a system becomes more localized with consequent drop and rise in S_r , S_p respectively. For the two family of states arising out of configurations (a) $1s n s \ ^3S$ ($n = 2-4$) and (b) $1s 3s \ ^3S$, $1s 3p \ ^3P$, $1s 3d \ ^3D$, in the intermediate and lower r_c region, the information entropies show interesting crossovers, and finally reach their free-atom limit at certain large r_c . In all cases, S_t bound is maintained. The emergence of these novel characteristics of S_r , S_p and S_t makes such information-centric analyses valuable tools for structure and dynamics under constrained environment. It would be worthwhile to extend the present study to the case of supposedly more realistic *penetrable* boundary. Besides we are also interested in several other information measures like Fisher information, Onicescu energy, Complexity etc., in such systems. Some of these works may be undertaken in future.

V. ACKNOWLEDGEMENT

SM is thankful to IISER Kolkata for a Senior Research Fellowship. Financial support from DAE BRNS, Mumbai (sanction order: 58/14/03/2019-BRNS) is gratefully acknowledged. Dr. Neetik Mukherjee is thanked for fruitful discussion. We thank the three anonymous referees for their valuable comments and suggestions.

-
- [1] W. Jaskólski. *Phys. Rep.*, 271:1, 1996.
 - [2] V. K. Dolmatov, A. S. Baltenkov, J.-P. Connerade, and S. T. Manson. *Radiat. Phys. Chem.*, 70:417, 2004.
 - [3] J. Sabin, E. Brändas, and S. Cruz (Eds.). *Adv. Quant. Chem.*, volume 57 & 58. Academic Press, New York, 2009.
 - [4] K. D. Sen (Ed.). *Electronic Structure of Quantum Confined Atoms and Molecules*. Springer International Publishing, Switzerland, 2014.
 - [5] E. Ley-Koo. *Revista Mexicana de Física*, 64:326, 2018.
 - [6] A. Michels, J. de Boer, and A. Bijl. *Physica*, 4:981, 1937.
 - [7] E. V. Ludeña. *J. Chem. Phys.*, 66:468, 1977.
 - [8] J. L. Marín and S. A. Cruz. *J. Phys. B*, 24:2899, 1991.
 - [9] S. Goldman and C. Joslin. *J. Phys. Chem.*, 96:6021, 1992.
 - [10] N. Aquino. *Int. J. Quant. Chem.*, 54:107, 1995.
 - [11] K. D. Sen, J. Garza, R. Vargas, and N. Aquino. *Phys. Lett. A*, 295:299, 2002.
 - [12] C. Laughlin, B. L. Burrows, and M. Cohen. *J. Phys. B*, 35:701, 2002.
 - [13] C. Laughlin. *J. Phys. B*, 37:4085, 2004.
 - [14] B. L. Burrows and M. Cohen. *Phys. Rev. A*, 72:032508, 2005.
 - [15] K. D. Sen and A. K. Roy. *Phys. Lett. A*, 357:112, 2006.
 - [16] B. L. Burrows and M. Cohen. *Int. J. Quant. Chem.*, 106:478, 2006.
 - [17] N. Aquino, G. Campoy, and H. E. Montgomery Jr. *Int. J. Quant. Chem.*, 107:1548, 2007.
 - [18] D. Baye and K. D. Sen. *Phys. Rev. E*, 78:026701, 2008.
 - [19] H. Ciftci, R. L. Hall, and N. Saad. *Int. J. Quant. Chem.*, 109:931, 2009.
 - [20] H. E. Montgomery Jr., and K. D. Sen. *Int. J. Quant. Chem.*, 109:688, 2009.

- [21] A. K. Roy. *Int. J. Quant. Chem.*, 115:937, 2015.
- [22] A. K. Roy. *Int. J. Quant. Chem.*, 116:953, 2016.
- [23] C. A. Ten Seldam and S. R. De Groot. *Physica*, 18:891, 1952.
- [24] E. V. Ludeña. *J. Chem. Phys.*, 69:1770, 1978.
- [25] J. Garza, J. M. Hernández-Pérez, J.-Z. Ramírez, and R. Vargas. *J. Phys. B*, 45:015002, 2012.
- [26] E. V. Ludeña and M. Gregori. *J. Chem. Phys.*, 71:2235, 1979.
- [27] R. Rivelino and J. D. M. Vianna. *J. Phys. B*, 34:L645, 2001.
- [28] C. Joslin and S. Goldman. *J. Phys. B*, 25:1965, 1992.
- [29] A. Banerjee, C. Kamal, and A. Chowdhury. *Phys. Lett. A*, 350:121, 2006.
- [30] A. Flores-Riveros, N. Aquino, and H. E. Montgomery Jr. *Phys. Lett. A*, 374:1246, 2010.
- [31] C. Le Sech and A. Banerjee. *J. Phys. B*, 44:105003, 2011.
- [32] T.-Y. Si, C.-G. Bao, and B.-W. Li. *Commun. Theor. Phys.*, 35:195, 2001.
- [33] H. E. Montgomery Jr., N. Aquino, and A. Flores-Riveros. *Phys. Lett. A*, 374:2044, 2010.
- [34] N. Aquino, A. Flores-Riveros, and J. F. Rivas-Silva. *Phys. Lett. A*, 307:326, 2003.
- [35] A. Flores-Riveros and A. Rodríguez-Contreras. *Phys. Lett. A*, 372:6175, 2008.
- [36] C. Laughlin and S. I. Chu. *J. Phys. A*, 42:265004, 2009.
- [37] C. L. Wilson, H. E. Montgomery Jr., K. D. Sen, and D. C. Thompson. *Phys. Lett. A*, 374:4415, 2010.
- [38] H. E. Montgomery Jr., and V. I. Pupyshev. *Phys. Lett. A*, 377:2880, 2013.
- [39] S. Bhattacharyya, J. K. Saha, P. K. Mukherjee, and T. K. Mukherjee. *Phys. Scr.*, 87:065305, 2013.
- [40] H. E. Montgomery Jr., and V. I. Pupyshev. *Theor. Chem. Acc.*, 134:1598, 2015.
- [41] J. Saha, S. Bhattacharyya, and T. K. Mukherjee. *Int. J. Quantum Chem.*, 116:1802, 2016.
- [42] Y. Yakar, B. Çakir, and A. Özmen. *Int. J. Quant. Chem.*, 111:4139, 2011.
- [43] S. B. Doma and F. N. El-Gammal. *J. Theor. Appl. Phys.*, 6:28, 2012.
- [44] A. Sarsa and C. Le Sech. *J. Chem. Theory Comput.*, 7:2786, 2011.
- [45] T. D. Young, R. Vargas, and J. Garza. *Phys. Lett. A*, 380:712, 2016.
- [46] V. I. Pupyshev and H. E. Montgomery Jr. *Theor. Chem. Acc.*, 136:138, 2017.
- [47] R. G. Parr and W. Yang. *Density Functional Theory of Atoms and Molecules*. Oxford University Press, New York, 1989.
- [48] C. Fiolhais, F. Nogueira, and M. Marques. *A Primer in Density Functional Theory*. Springer,

- Berlin, 2003.
- [49] E. Engel and R. M. Dreizler. *Density Functional Theory: An Advance Course (Theoretical and Mathematical Physics)*. Springer, New York, 2011.
- [50] A. D. Becke. *Phys. Rev. A*, 38:3098, 1988.
- [51] J. Garza, R. Vargas, and A. Vela. *Phys. Rev. E*, 58:3949, 1998.
- [52] F.-A. Duarte-Alcaráz, M.-A. Martínez-Sánchez, M. Rivera-Almazo, R. Vargas, R.-A. Rosas-Burgos, and J. Garza. *J. Phys. B*, 52:135002, 2019.
- [53] N. Aquino, A. Flores-Riveros, J. F. Rivas-Silva, and K. D. Sen. *J. Chem. Phys.*, 124:054311, 2006.
- [54] J. P. Perdew and Y. Wang. *Phys. Rev. B*, 45:13244, 1992.
- [55] S. Waugh, A. Chowdhury, and A. Banerjee. *J. Phys. B*, 43:225002, 2010.
- [56] S. F. Vyboishchikov. *J. Comput. Chem.*, 36:2037, 2015.
- [57] M. Lozano-Espinosa, J. Garza, and M. Galván. *Phil. Mag.*, 97:284, 2017.
- [58] S. F. Vyboishchikov. *J. Comput. Chem.*, 37:2677, 2016.
- [59] S. F. Vyboishchikov. *ChemPhysChem*, 18:3478, 2017.
- [60] Meta van Faassen. *J. Chem. Phys.*, 131:104108, 2009.
- [61] C. E. Shannon. *Bell Sys. Tech. J.*, 30:50, 1951.
- [62] I. Bialynicki-Birula and J. Mycielski. *Commun. Math. Phys.*, 44:129, 1975.
- [63] J.-H. Ou and Y. K. Ho. *Int. J. Quantum Chem.*, 119:e25928, 2019.
- [64] K. D. Sen. *J. Chem. Phys.*, 123:074110, 2005.
- [65] L. G. Jiao, L. R. Zan, Y. Z. Zhang, and Y. K. Ho. *Int. J. Quant. Chem.*, 117:e25375, 2017.
- [66] N. Mukherjee and A. K. Roy. *Int. J. Quant. Chem.*, 118:e25596, 2018.
- [67] N. Mukherjee and A. K. Roy. *Eur. Phys. J. D*, 72:118, 2018.
- [68] N. Aquino, A. Flores-Riveros, and J. F. Rivas-Silva. *Phys. Lett. A*, 377:2062, 2013.
- [69] S. A. Cruz, C. Díaz-García, H. Olivares-Pilón, and R. Cabrera-Trujillo. *Radiat. Effects & Defects in Solids*, 171:123, 2016.
- [70] J.-H. Ou and Y. K. Ho. *Atoms*, 5:15, 2017.
- [71] J.-H. Ou and Y. K. Ho. *Chem. Phys. Lett.*, 689:116, 2017.
- [72] M. Rodriguez-Bautista, R. Vargas, N. Aquino, and J. Garza. *Int. J. Quant. Chem.*, 118:e25571, 2018.
- [73] M.-A. Martínez-Sánchez, R. Vargas, and J. Garza. *Quantum Rep.*, 1:208, 2019.

- [74] J. P. Restrepo Cuartas and J. L. Sanz-Vicario. *Phys. Rev. A*, 91:052301, 2015.
- [75] G. Brual and S. M. Rothstein. *J. Chem. Phys.*, 69:1177, 1978.
- [76] C. Lee, Y. Wang, and R. G. Parr. *Phys. Rev. B*, 37:785, 1988.
- [77] A. K. Roy, R. Singh, and B. M. Deb. *J. Phys. B*, 30:4763, 1997.
- [78] A. K. Roy, R. Singh, and B. M. Deb. *Int. J. Quant. Chem.*, 65:317, 1997.
- [79] A. K. Roy and B. M. Deb. *Phys. Lett. A*, 234:465, 1997.
- [80] A. K. Roy and S. I. Chu. *Phys. Rev. A*, 65:052508, 2002.
- [81] A. K. Roy. *J. Phys. B*, 37:4369, 2004.
- [82] A. K. Roy. *J. Phys. B.*, 38:1591, 2005.
- [83] A. K. Roy and A. F. Jalbout. *Chem. Phys. Lett.*, 445:355, 2007.
- [84] V. Sahni and M. Harbola. *Int. J. Quant. Chem. Symp.*, 24:569, 1990.
- [85] V. Sahni, Y. Li, and M. Harbola. *Phys. Rev. A*, 45:1434, 1992.
- [86] A. K. Roy. *Phys. Lett. A*, 321:231, 2004.
- [87] A. K. Roy. *J. Phys. G*, 30:269, 2004.
- [88] A. K. Roy. *Pramana-J. Phys.*, 38:2189, 2005.
- [89] A. K. Roy. *Int. J. Quant. Chem.*, 104:861, 2005.
- [90] S. R. Gadre, S. B. Sears, S. J. Chakravorty, and R. D. Bendale. *Phys. Rev. A*, 32:2602, 1985.
- [91] C. Amovilli and F. M. Floris. *Computation*, 6:36, 2018.
- [92] C.-H. Lin and Y. K. Ho. *Chem. Phys. Lett.*, 633:261, 2015.
- [93] J.-H. Ou and Y. K. Ho. *Atoms*, 7:70, 2019.
- [94] N. L. Guevara, R. P. Sagar, and R. O. Esquivel. *J. Chem. Phys.*, 119:7030, 2003.